# Analysis of Active Site Residues of Botulinum Neurotoxin E by Mutational, Functional, and Structural Studies: Glu335Gln Is an Apoenzyme†

Rakhi Agarwal,‡ Thomas Binz,§ and Subramanyam Swaminathan*,‡

*Biology Department, Brookhaven National Laboratory, Upton, New York 11973, and Department of Biochemistry, Medizinische Hochschule Hannover, Hannover, Germany*

*Received February 10, 2005; Revised Manuscript Received April 18, 2005*

ABSTRACT: Clostridial neurotoxins comprising the seven serotypes of botulinum neurotoxins and tetanus neurotoxin are the most potent toxins known to humans. Their potency coupled with their specificity and selectivity underscores the importance in understanding their mechanism of action in order to develop a strategy for designing counter measures against them. To develop an effective vaccine against the toxin, it is imperative to achieve an inactive form of the protein which preserves the overall conformation and immunogenicity. Inactive mutants can be achieved either by targeting active site residues or by modifying the surface charges farther away from the active site. The latter affects the long-range forces such as electrostatic potentials in a subtle way without disturbing the structural integrity of the toxin causing some drastic changes in the activity/environment. Here we report structural and biochemical analysis on several mutations on *Clostridium botulinum* neurotoxin type E light chain with at least two producing dramatic effects: Glu335Gln causes the toxin to transform into a persistent apoenzyme devoid of zinc, and Tyr350Ala has no hydrolytic activity. The structural analysis of several mutants has led to a better understanding of the catalytic mechanism of this family of proteins. The residues forming the S1′ subsite have been identified by comparing this structure with a thermolysin−inhibitor complex structure.

Clostridial neurotoxins comprising seven antigenically different botulinum neurotoxins (BoNTs)[1] and the tetanus neurotoxin (TeNT) are unique zinc endopeptidases. They all share significant sequence homology and structural and functional similarities and cleave one of the three proteins of the SNARE complex required for docking and fusion with target membranes for neurotransmitter release (*1*). Cleavage of any one of the SNARE proteins inhibits the exocytosis of neurotransmitters causing paralysis (*2*). Neurotoxins are unique since they cleave specific substrates precisely at a particular peptide bond. What confers this unique property is still not understood which is essential if a common therapeutic agent is to be developed for all of them since they are considered potential biowarfare threats. The active sites of the catalytic domains of at least four of them have been analyzed crystallographically (*3*−*7*).

Various serotypes of botulinum neurotoxins share nearly 32% sequence identity and 53% similarity (*8*, *9*). A comparison of the catalytic domains of botulinum neurotoxins for which experimental structures are available shows a deep cavity through which substrates could access the active site. Despite high sequence and structural similarity each serotype has a specific substrate and cleavage site selectivity. This suggests that the enzyme has unique recognition site(s) that help(s) in the substrate binding and docking leading to ultimate cleavage of the scissile bond. The recognition site is presumably the SSR sequence (SNARE secondary recognition) motifs present in each neuronal synaptic vesicle fusion protein (*10*). The specificity of the botulinum neurotoxins toward the SSR sequence is very low, and almost each one is able to bind to all SSR sequences irrespective of substrate specificity (*10*). However, each serotype requires a minimum length of the substrate which includes a SSR sequence for the optimum activity (*11*, *12*). The clostridial neurotoxin substrate specificity could also be dictated by the complementarity between the substrate and the enzyme.

The active site of botulinum neurotoxins is comprised of the HExxH+E zinc-binding motif. In the case of BoNT/E-LC His211, His215, and Glu250 directly coordinate with zinc, and a nucleophilic water hydrogen bonded to Glu212 acts as the fourth ligand (*3*). The general conformation and the active site residues are conserved in all clostridial neurotoxins.

Mutational studies have been carried out extensively on BoNT/A and TeNT-LC (*13*−*16*). The effect of mutating residues Arg362, Tyr365, and Glu350 in BoNT/A on the proteolytic activity has been studied (*13*, *14*). It was also established that Glu224Gln completely abolishes the activity in BoNT/A; Glu224, though not directly coordinated to zinc, is hydrogen bonded to the nucleophilic water coordinated to zinc (*17*). Mutational studies on thermolysin, a metallo-

† Research supported by the U.S. Army Medical Research Acquisition Activity (Award No. DAMD17-02-2-0011) under DOE Prime Contract No. DE-AC02-98CH10886 with Brookhaven National Laboratory. T.B. was supported by Grant RGY0027/2001 from the Human Frontier Science Program.

* To whom correspondence should be addressed. E-mail: swami@bnl.gov. Telephone: (631) 344-3187. Fax: (631) 344−3407.

‡ Brookhaven National Laboratory.

§ Medizinische Hochschule Hannover.

[1] Abbreviations: BoNT, botulinum neurotoxin; TeNT, tetanus neurotoxin; SNARE, soluble NSF attachment protein receptor; SSR, SNARE secondary recognition; LC, light chain; SNAP-25, 25 kDa synaptosome-associated protein; PMSF, phenylmethanesulfonyl fluoride; HEPES, *N*-(2-hydroxyethyl)piperazine-*N*′-2-ethanesulfonic acid.

10.1021/bi050253a CCC: $30.25 
Published on Web 05/19/2005

Table 1: Complementary Primer Sequences Designed and Used for Generating the Different Mutations in BoNT/E-LC

| mutation | primer sequence |
|---|---|
| Glu249Ala | F: 5′-CAAATATAAGAGGTACAAATATTGCAGAGTTCTTAACTTTTGGAG-3′ |
| | R: 5′-CTCCAAAAGTTAAGAACTCTGCAATATTTGTACCTCTTATATTTG-3′ |
| Tyr350Ala | F: 5′-GTTAAATGTAGGCAAACTGCCATTGGACAGTATAAATACTTCAAACTTTC-3′ |
| | R: 5′-GAAAGTTTGAAGTATTTATACTGTCCAATGGCAGTTTGCCTACATTTAAC-3′ |
| Arg347Ala | F: 5′-CTAAATTTCAAGTTAAATGTGCGCAAACTTATATTGGACAG-3′ |
| | R: 5′-CTGTCCAATATAAGTTTGCGCACATTTAACTTGAAATTTAG-3′ |
| Glu335Ala | F: 5′-ATTATACAGCTTTACGGCATTCGATTTAGCAACTAAATTT-3′ |
| | R: 5′-AAATTTAGTTGCTAAATCGAATGCCGTAAAGCTGTATAAT-3′ |
| Glu335Gln | F: 5′-ATTATACAGCTTTACGCAATTTGATTTAGCAACTAAATTT-3′ |
| | R: 5′-AAATTTAGTTGCTAAATCAAATTGCGTAAAGCTGTATAAT-3′ |
| Glu158Ala/Thr159Ala/Asn160Ala | F: 5′-TAGAGAAATATTGGAACTGGCAGCTGCAAATAAATCAGGCTCTGC-3′ |
| | R: 5′-GCAGAGCCTGATTTATTTGCAGCTGCCAGTTCCAATATTTCTCTA-3′ |

protease whose active site geometry is very similar to botulinum neurotoxins and neprilysin, a related protein, have also been reported. Both of them contain the same kind of zinc-binding motif. Residues His231 and His711 of thermolysin and neprilysin play a crucial role in substrate stabilization (*18*−*21*). In addition, there are other residues which may have corresponding residues in BoNTs. The catalytic mechanism of these two proteins and botulinum neurotoxins appears to be similar with some differences.

A structural comparison of at least three serotypes reveals several conserved residues at/near the active site of the enzymes (*3*) and also at distances >10 Å from the active site zinc. Since the catalytic activity and the kinetic parameters of an enzyme rely on the charged groups present in the active site stabilizing the transition state as acid or base catalysts in the reaction, it is possible to modify the catalytic activity by changing the properties of the active site residues without structural alteration. The proteolysis also depends on the intricate electrostatic potential developed by short-range effects such as hydrogen bonds or hydrophobic interactions, as well as long-range interactions. It is difficult to explain fully the change in the electrostatic interactions due to change in amino acid residues in a protein in an electrostatic model without accounting for all possible parameters contributing to dynamics of the protein (*22*). Accordingly, a major part of the enzyme may be involved in optimizing the catalytic center.

A mutational study on Glu212 has been reported for BoNT/E-LC (*3*). In the same study, several residues in the active site and their interactions with other residues that will be common in all clostridial neurotoxins were pointed out. This report focuses mainly on mutation of some of these residues. These are Glu158Ala/Thr159Ala/Asn160Ala (a triple mutant), Glu249Ala, Glu335Ala, Glu335Gln, Glu212Gln/Glu335Gln (a double mutant), Arg347Ala, and Tyr350Ala. We have analyzed the functional role of these residues systematically by mutating one residue at a time and in combination and by determining the three-dimensional structures of five mutants (Glu158Ala/Thr159Ala/Asn160Ala, Glu335Ala, Glu335Gln, Arg347Ala, and Tyr350Ala) to understand the conformational or other environmental changes in the active site to establish structure−function correlation. Since these residues are mostly conserved, we can define their roles in all serotypes by extension.

## EXPERIMENTAL PROCEDURES

*Site-Directed Mutagenesis.* The complementary PCR primers (Invitrogen) were designed for the missense mutations Glu158Ala/Thr159Ala/Asn160Ala, Glu249Ala, Glu335Ala, Glu335Gln, Arg347Ala, and Tyr350Ala (Table 1). The native pET-9c-LC (*23*) was used as template along with the Quick-Change site-directed mutagenesis kit (Stratagene, La Jolla, CA) for mutagenesis according to the manufacturer's manual. The double mutant Glu212Gln/Glu335Gln was generated with Glu212Gln mutant DNA template and the primers of Glu335Gln mutation. To confirm the mutations, the entire region encoding the mutated light chain (LC) was sequenced in both of the strands using the Big Dye terminator cycle sequencing (Applied Biosystems) method.

*Expression and Purification of the BoNT/E-LC Mutant Proteins.* The plasmid DNAs were transfected into *Escherichia coli* BL21(DE3) bacteria for the expression of the protein. The growth conditions of the culture for expression and the method of purification of the protein are as for the wild-type protein (*23*).

The 2×YT medium (1.6% bactotryptone, 1.0% bacto-yeast extract, and 0.5% NaCl) was used to grow the cells at 37 °C with shaking until the $A_{600}$ reached 0.6. IPTG (1 mM) was added at this point, and cells were incubated at 20 °C for an additional 12 h. The induced cells were pelleted down by centrifugation at 5000 rpm at 4 °C for 10 min. The cell pellet was suspended in 20 mL of lysis buffer (50 mM sodium phosphate, pH 8.0, 300 mM NaCl, 5 mM benzamidine, 0.5 mM PMSF, 1 μg/mL pepstatin A) supplemented with two tablets of protease inhibitor cocktail (Roche), 2 mL of Bugbuster (Novagen), 6 mM iodoacetamide, and 2 μL of Benzonase (Novagen) and incubated at room temperature for 20 min. The lysate was centrifuged at 16500 rpm for 30 min to remove insoluble cell debris. The protein was purified using a Ni-NTA agarose (Qiagen) column and elution with increasing concentrations of imidazole (10−250 mM). Further purification of wild type and mutants was done by size-exclusion chromatography (Superdex-75) employing the Akta-Prime purifier system (Amersham). The buffer was also exchanged from phosphate to HEPES buffer (20 mM HEPES, pH 7.2, 200 mM NaCl) in this process. Proteins were stored at −70 °C until used. A high-level expression of protein has been achieved (>15 mg/500 mL of culture).

*Construction of N- and C-Terminal 6×-His-Tagged SNAP-25.* The pET28-b vector which has a 6×-His tag at both N- and C-terminal ends has been used. The PCR amplification of the SNAP-25 gene using the pGEX-2T-SNAP-25 vector (kindly provided by Dr. Eric Johnson, University of Wisconsin) as template was performed using the following primers: forward, 5′ CCG CGT **GCT AGC** ATG GCC GAG G 3′, and reverse, 5′ GGC A**CT CGA G**AC CAC

Table 2: Data Collection and Refinement Statistics

| | E335Q | E335A[a] | R347A[a] | triple mutant | Y350A |
|---|---|---|---|---|---|
| crystal data | | | | | |
| *a*, *b*, *c* (Å)[b] | 88.8(1), 144.6(2), 83.31(1) | | | | |
| space group | $P2_12_12$ | | | | |
| PDB ID code | 1ZL5 | 1ZN3 | 1ZKW | 1ZKX | 1ZL6 |
| resolution (Å) | 50−2.6 | 50−2.6 | 50−1.93 | 50−2.5 | 50−2.4 |
| no. of reflections | 30978 | 34510 | 72275 | 36986 | 42956 |
| $I/\sigma$[c] | 5.8 (2) | 9.0 (3) | 6.4 (2) | 5.4 (2) | 9.0 (3) |
| $R_{merge}$[d] | 0.12 (0.43) | 0.11 (0.50) | 0.09 (0.50) | 0.07 (0.42) | 0.08 (0.43) |
| redundancy | 6.9 | 6.6 | 5.0 | 7.3 | 5.9 |
| refinement statistics | | | | | |
| resolution (Å) | 50−2.6 | 50−2.6 | 50−2.2 | 50−2.5 | 50−2.4 |
| no. of reflections | 28511 | 32370 | 49723 | 26893 | 38653 |
| completeness (%) | 84.3 (55.3) | 95.7 (95) | 96 (82.4) | 74 (54.7) | 90 (89) |
| *R*-factor[e] | 0.20 | 0.22 | 0.23 | 0.20 | 0.23 |
| $R_{free}$ | 0.27 | 0.26 | 0.28 | 0.25 | 0.28 |
| no. of protein atoms | 6563 | 6463 | 6571 | 6545 | 6305 |
| no. of heteroatoms | 9 | 7 | 9 | 6 | 3 |
| no. of water molecules | 250 | 350 | 263 | 244 | 207 |
| RMSD bonds | 0.007 | 0.008 | 0.007 | 0.007 | 0.007 |
| RMSD angles | 1.34 | 1.40 | 1.29 | 1.33 | 1.29 |
| Ramachandran plot | | | | | |
| most favored (%) | 85 | 85 | 85 | 84 | 85 |
| additionally allowed (%) | 14 | 14 | 14 | 15 | 15 |

[a] Outermost shell reflections not included for refinement. [b] Mean values for the five structures are given. [c] Values within parentheses are for the outermost shell. [d] $R_{merge} = \sum_j(|I_h - \langle I\rangle_h|)/\sum I_h$, where $\langle I_h\rangle$ is the mean intensity of reflection *h*. [e] *R*-factor $= \sum|F_o - F_c|/\sum|F_o|$.

TTC CCA GC 3′ (the underlined sequence represents *Nhe*I and *Xho*I restriction sites). The PCR sample and the vector were digested with the same restriction enzymes and were ligated together using the T4-ligation system (New England Biolabs). The clone was confirmed for the correct sequence by DNA sequencing of both of the strands by the Big Dye terminator cycle sequencing (Applied Biosystems) method.

*Expression and Purification of SNAP-25.* The pET28-b-SNAP-25 clone was transformed to *E. coli* BL21(DE3) cells and expressed. The purification protocol is the same as for BoNT/E-LC (*23*). The protein is stable for more than 6 months when stored between −80 and −20 °C. On a native gel the protein showed a band corresponding to ∼52 kDa, suggesting it to be a dimer in solution. On SDS−PAGE gel it shows the expected ∼26 kDa size. The total recovery of protein was found to be ∼20 mg/L of culture.

*Enzymatic Activity of Wild-Type vs Mutant Proteins.* The proteolytic activity of the wild type and mutants of BoNT/E-LC was assayed in vitro on its substrate SNAP-25. The assay was performed in a final volume of 20 μL of activity assay buffer (20 mM HEPES, pH 7.4, 2 mM DTT) containing 2 nM concentration of LC and 7 μM concentration of SNAP-25 at 37 °C for 60 min. Trials were carried out with and without zinc acetate in the assay buffer. Since the difference was marginal or none, the results reported here are with assay buffer devoid of zinc acetate. However, the mutant protein concentration in the reaction mixture was varied in another experiment from 5 to 500 nM, since at 2−5 nM some of the mutants did not exhibit any hydrolytic activity. Here, the cleavage of SNAP-25 by the LCs was determined by incubating the samples at 37 °C for 20 min. The reactions were stopped by adding 10 μL of 3× concentrated SDS−PAGE sample buffer containing 1 mM EDTA to chelate the Zn cofactor, if present. The extent of cleavage was then evaluated following electrophoresis on 4−20% Tris−glycine SDS−PAGE gels (Cambrex) by the appearance and intensity of a new band at ∼23 kDa due to the cleavage of SNAP-25 between aa 180 and 181. The cleaved and uncleaved substrate fractions were quantified using densitometry, and the kinetic parameters were derived using Lineweaver−Burk plots.

*Binding Assay of Mutants.* To ascertain that the mutant's reduced or loss of catalytic activity is not due to their inability to bind to the substrate, a binding assay was performed. The wild-type enzyme and the mutants were mixed in 1:1 ratio and then incubated with SNAP-25 in 1:1000 ratio in the activity assay buffer for 15 min at 37 °C. As a control, the same experiment was repeated with the wild-type enzyme premixed with an unrelated protein BSA or lysozyme. All of the reactions were stopped and run on SDS−PAGE gels to compare the results.

*Crystallization and Data Collection of Glu335Gln, Glu335Ala, Arg347Ala, Tyr350Ala, and Glu158Ala/Thr159Ala/Asn160Ala Mutants.* Crystallization screening was carried out by the sitting drop vapor diffusion method using Hampton Research crystallization screens. Diffraction quality crystals were obtained at room temperature using 0.5 M ammonium sulfate, 1.0 M $Li_2SO_4$ and 0.1 M sodium citrate trihydrate at pH 5.6 as precipitant, and crystals grew to their full size in 2−6 days. Crystals belong to the space group $P2_12_12$, same as wild type (*23*). The cell parameters for crystals of mutant proteins and wild-type LC are similar.

Diffraction data from crystals of mutants were collected at the NSLS beamlines. Crystals were briefly transferred to the mother liquor containing 20% glycerol and were mounted on a nylon loop and flash frozen immediately by plunging into liquid nitrogen. Data covering at least 180° rotation in $\phi$ were collected, for an oscillation range of 1° per frame at $\lambda = 1.1$ Å. Data were processed, scaled, and merged with HKL2000 (*24*). Details of data collection statistics are given in Table 2.

*Structure Determination of Mutant Proteins.* Since the mutant crystals were isomorphous to the wild type, the BoNT/E-LC model (PDB ID 1T3A) with appropriate muta-

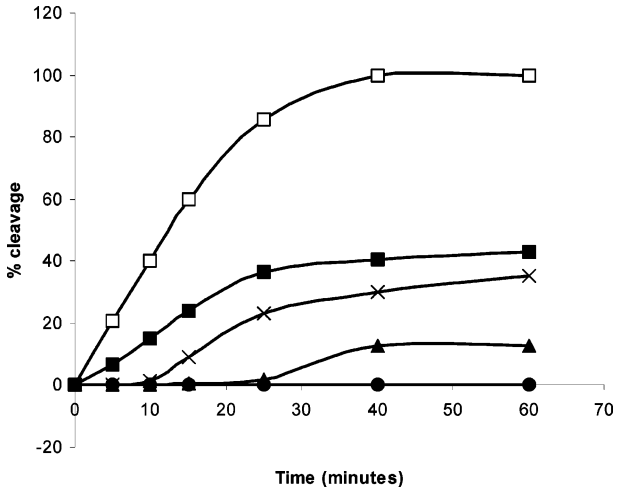


FIGURE 1: Catalytic activity of wild-type BoNT/E-LC and various mutants. The cleavage values were determined in a total volume of 20 $\mu$L at 37 °C using 7 $\mu$M N- and C-terminal 6×-His-tagged SNAP-25 with 2 nM light chain concentrations. At indicated time intervals aliquots were removed and analyzed on SDS−PAGE gels and with Coomassie blue staining. The quantity of protein was determined using densitometry analysis. The data represent the average of three independent experiments: wild type (□), triple mutant (■), Glu249Ala (×), Glu335Ala (▲) and Arg347Ala, Tyr350Ala, Glu335Gln, and Glu212Gln/Glu335Gln double mutant (●).

tion was used as the starting model. After initial rigid body refinement, the model was refined by simulated annealing using CNS (*25*). Solvent molecules were added also using CNS. Composite omit maps were computed and used to fine-tune the model without model bias using the program O (*26*). The refinement statistics are included in Table 2.

## RESULTS AND DISCUSSION

*Enzymatic Activity of Wild-Type and Various Mutant Proteins.* The hydrolytic activities of the wild-type and mutant proteins at the same concentration are shown in Figure 1. Triple mutant and Glu249Ala showed ~43% and 36% activity as compared to wild type, whereas Tyr350Ala, Arg347Ala, and Glu335Gln failed to show any activity in that particular experiment. Glu335Ala showed ~13% activity with respect to wild type.

In another experiment, various concentrations of the mutant proteins (5−500 nM) were used on 7 $\mu$M substrate with a fixed time interval (20 min) at 37 °C (data not shown). Wild type could digest the substrate completely at 5 nM enzyme concentration, while Tyr350Ala did not show any activity even at a 500 nM level. For Glu335Gln and Arg347Ala mutants there was no activity up to 50 nM, but residual activity started appearing at 500 nM enzyme concentration with about <5% and 20% of the substrate cleaved, respectively. While the Glu335Ala mutant started showing activity at 50 nM, other mutants such as Glu249Ala and the triple mutant had detectable activity even at 5 nM concentration.

*Kinetic Studies for the Wild-Type and Various Mutant Proteins.* The enzyme kinetic values were determined by the cleavage rate of SNAP-25 at different concentrations. The derived $K_m$ and $K_{cat}$ values are shown in Table 3. The values for the wild type are slightly different from what we had reported earlier (*23*). This may be because we had used

Table 3: Enzyme Kinetic Parameters of the Wild-Type BoNT/E-LC and Various Mutants

| light chains | $K_m$ ($\mu$M) | $K_{cat}$ (min$^{-1}$) | $K_{cat}/K_m$ ($\mu$M$^{-1}$ min$^{-1}$) |
|---|---|---|---|
| wild type | 7.9 ± 0.4 | 257.11 ± 21 | 32.75 |
| Glu335Gln | 10 ± 0.5 | 0.045 ± 0.003 | 0.0045 |
| Glu335Ala | 9.7 ± 0.8 | 8.66 ± 0.2 | 0.89 |
| Tyr350Ala | not detectable | not detectable | not detectable |
| Arg347Ala | 11.2 ± 0.2 | 0.35 ± 0.045 | 0.031 |
| triple mutant | 11.3 ± 1.0 | 50.17 ± | 4.43 |
| Glu249Ala | 11.2 ± 2.0 | 24.17 ± 5.9 | 1.62 |
| Glu212Ala/ Glu335Gln | not detectable | not detectable | not detectable |

SNAP-25 with a GST tag earlier while we are using SNAP-25 with an N- and C-terminal 6×-His tag now. For mutants the assay was repeated by adding (an increasing amount of) zinc acetate (50−100 $\mu$M) to the reaction buffer, but this had no effect on the activity.

Two of the mutations with drastic effect on the activity are Tyr350Ala, which failed to show any activity, and Glu335Gln, with ~7000-fold less $K_{cat}/K_m$ than wild type. However, substitution of Glu335 to Ala reduced the $K_{cat}/K_m$ by ~40-fold only. The $K_m$ values for all of the mutants were only marginally higher than that for the wild type, suggesting similar affinity to the substrate. Any change in activity was due to changes in the $K_{cat}$ values. However, $K_m$ for Tyr350Ala could not be determined. Another severe phenotype was exhibited by the Arg347Ala mutant, which has ~1000-fold lower catalytic efficiency than the wild type. On the basis of severity phenotype the mutants in this study can be ordered as Glu335Gln/Glu212Gln and Tyr350Ala > Glu335Gln > Arg347Ala > Glu335Ala > Glu249Ala > triple mutant.

*Substrate Binding Assay for Mutant Proteins.* The substrate binding assay for the various mutants such as Arg347Ala, Tyr350Ala, Glu335Gln, and Glu212Gln/Glu335Gln showed that they compete for binding to the substrate with the wild-type enzyme (data not shown). This is also supported by the $K_m$ values of the hydrolytically active (at least to some extent) mutants, which are similar to the wild-type value.

*Structural Description of Various Mutants.* In general, there is no global conformational change in any of the mutants compared to the wild-type structure (Figure 1 in ref *3*) except for some side chain orientation and the position of nucleophilic water at the active site. A few extra residues appear in the loop regions for some mutant structures, which is not uncommon. Description and discussion of each structure follows.

*(A) Arg347Ala.* Arg347 was selected for the study since this residue has been implicated in catalytic activity both by a mutagenesis study (BoNT/A) and by similarity to thermolysin Arg203 (*13*, *18*−*21*, *27*). In BoNT, Arg347 is in the secondary coordination sphere of zinc. Glu335 acts as a bridge between Arg347 and His211 and is hydrogen bonded to them, stabilizing the active site (*3*). It is possible that any perturbation in this interaction might affect the active site architecture and, consequently, the activity. However, the terminal nitrogen atoms of the guanidino group of Arg347 are more than 7 Å away from either zinc or nucleophilic water in BoNTs. The active site geometry is almost preserved in the Arg347Ala mutant structure. The coordination of zinc remains the same except that the nucleophilic water has

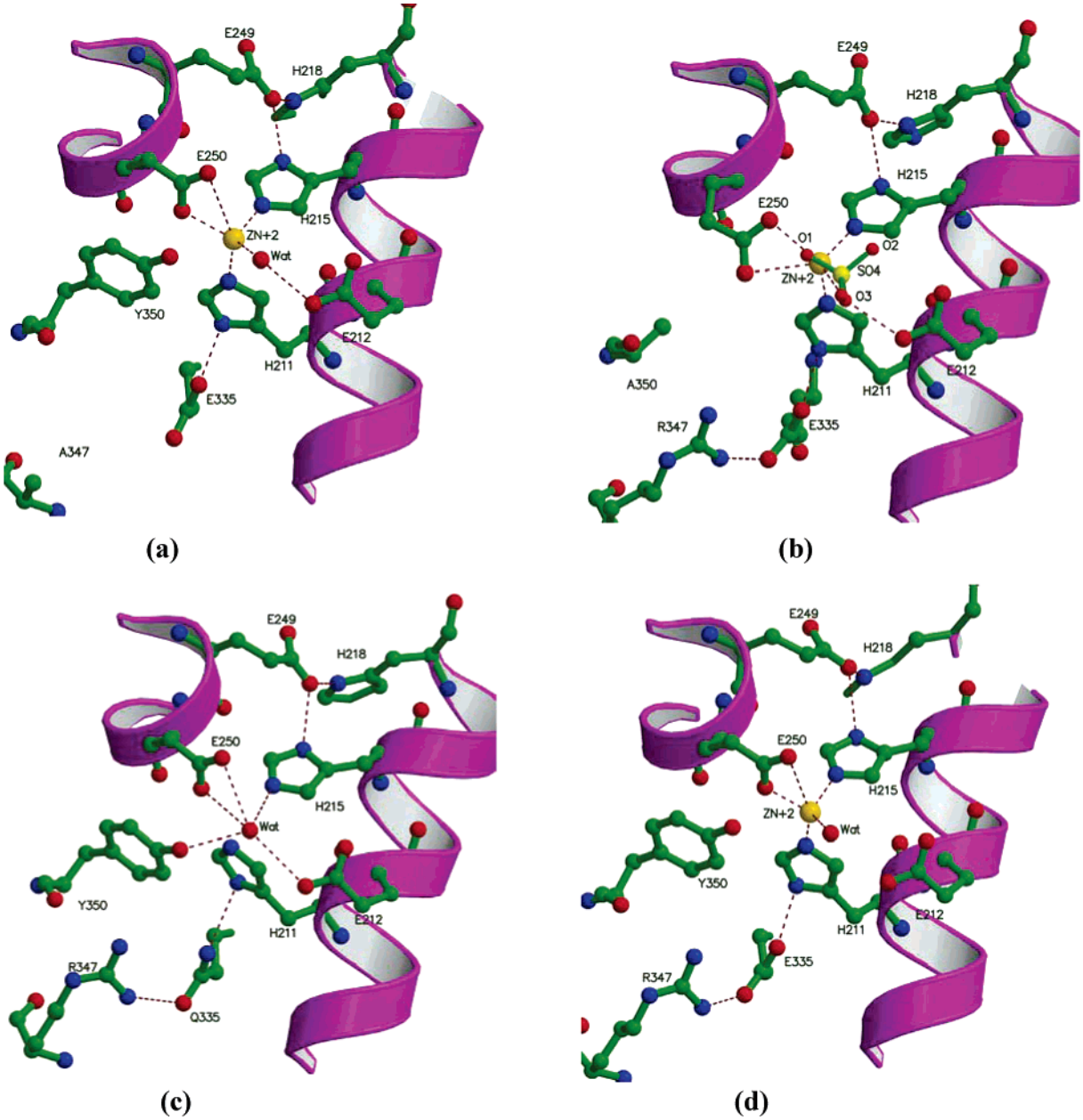


FIGURE 2: Active site of the four mutants: (a) Arg347Ala, (b) Tyr350Ala, (c) Glu335Gln, and (d) Glu158Ala/Thr159Ala/Asn160Ala triple mutant. Carbon, nitrogen, and oxygen atoms are shown as spheres in green, dark blue, and red. Zinc is in yellow, and dashed lines represent coordination and hydrogen bond contacts. For Tyr350Ala, the active site of molecule B is given. All distances are given in Table 4. These figures were generated with MOLSCRIPT and Raster3D (*34*).

moved away to 2.6 Å, changing from coordination to hydrogen bonding distance (Figure 2a). It was expected that the loss of hydrogen-bonding interaction between Arg347 and Glu335 would affect the hydrogen bond contact between Glu335 and His211. However, this hydrogen bond is intact, and the orientation of His211 is unaltered and similar to that of the wild-type structure (*3*).

*(B) Tyr350Ala.* Mutation of the residue equivalent to Tyr350 has been studied both in BoNT/A and in TeNT (*13*−*15*). When it was substituted with Phe, there was 25−30% residual activity in both BoNT/A and TeNT. Mutation with Ala had different effects in BoNT/A and TeNT. While the activity was completely lost in TeNT (*15*), about 20−30% was retained in BoNT/A (*14*). In BoNT/E-LC the effect is similar to that of TeNT, and the activity is barely detectable even at high concentration (5 $\mu$M) of the mutant enzyme (Tyr350Ala).

As in the case of Arg347Ala, the conformation of the active site remains almost the same. The coordination distance between zinc and histidines is not changed. However, as a consequence of the loss of the phenolic ring and hence the aromatic−anionic interaction stabilizing the position of Glu250, the side chain of Glu250 takes a different rotamer position and moves closer to the original position of the Tyr350 side chain. It also increases the distance between zinc and the carboxylate group of Glu250 (molecule A). Interestingly, in the crystal structure of Tyr350Ala a sulfate ion replaces the nucleophilic water in molecule A similar to that observed in the BoNT/B holotoxin structure (*28*). The sulfate ion may have been incorporated during crystallization, since ammonium and lithium sulfates were present in the crystallization condition (Figure 2b).

The nucleophilic water is intact in molecule B of the LC dimer, though displaced to 3.21 Å from zinc. It moves closer

to Glu212 and is at a distance of 2.42 Å, making a very strong hydrogen bond. This is similar to movement of the water during the transition state, allowing the scissile carbonyl carbon to form a tetrahedral geometry (*29*). This movement of water closer to Glu212 is because of the loss of interaction between Tyr350 OH and the nucleophilic water that was present in the wild-type structure. This may be one reason a sulfate ion is able to displace the water in molecule A of Tyr350Ala unlike other BoNT/E structures where the water is tightly kept in position by tyrosine even though the crystallization conditions are the same. The packing consideration could have prevented the replacement of water in molecule B.

*(C) Glu335Ala.* Residues Glu249 and Glu335 are in the secondary coordination sphere in clostridial neurotoxins. Glu249 helps in positioning and orienting His215 for coordination with zinc, while Glu335 does the same for His211. In addition, these two are charged amino acids and are about 8 Å away from the zinc. As in the case of Glu212, changing them to nonconservative residues might alter the electrostatic potential near the zinc atom affecting the catalytic activity significantly. The Glu249Ala mutation caused the activity to decrease 15-fold. Glu249 is a conserved residue in all BoNTs except in serotype C. In the case of serotype C this residue is an alanine, and not surprisingly BoNT/C is less active than other BoNTs (*11*). However, the structure of Glu249Ala was not determined.

The crystal structure of Glu335Ala is similar to the wild type except for some minor changes in the side chain conformation of the active site residues. As in the case of Arg347Ala, the nucleophilic water has moved away from the active site zinc closer to Glu212. Active site zinc is intact, and the orientation of His211 is unaltered. A strong residual density persisted in the difference Fourier map and was modeled as chlorine because of its location. Interestingly, this chlorine ion is bridging the side chains of His211 and Arg347. In molecule B, this chlorine ion may be disordered as also the nucleophilic water.

*(D) Glu335Gln.* Interestingly, when Gln replaces Glu (Glu335Gln) there was a drastic drop in catalytic efficiency (~7000-fold). Though the active site geometry remained the same, it was devoid of zinc (Figure 2c). Neither the composite omit map nor the difference Fourier computed with the final model showed any electron density at the expected zinc position (Figure 3). Though we did not determine the zinc content by spectroscopic experiments, we routinely scan the crystal (in this case even the protein at 10 mg/mL) near the absorption edge of zinc at the synchrotron beamline during X-ray diffraction data collection. While wild type and other mutants gave a good signal near the zinc absorption edge (9659 eV), Glu335Gln and Glu212Gln/Glu335Gln were noisy with no detectable signal. Glu335 makes hydrogen bonds with Arg347 and His211 in the wild-type structure. Though the type of contacts may be different, Gln335 also makes hydrogen bonds with both Arg347 and His211 (significantly longer than wild type, Table 4), but the orientation of His211 has changed ($\chi_2$ by 20°) and probably its protonation state also. It is intriguing that the nucleophilic water is still present, though moved away from the original position by about 0.8 Å (Figure 4a). It makes strong hydrogen bonds with His215, Glu250, and Glu212 and also with Tyr350 (Table 4). This suggests that the nucleophilic water is compensating for the loss of the zinc ion by interacting more closely with these residues. This is similar to the apo BoNT/B structure, though in apo BoNT/B, Glu267 (corresponding to Glu250 of BoNT/E) had taken a different rotamer position from the holotoxin moving closer to Gln264 (*30*). In BoNT/E-LC, the position and orientation of Glu250 are unaltered, but both of the carboxylate oxygens make strong hydrogen bonds with the nucleophilic water. A similar water molecule has been observed in the apo BoNT/B crystal structure also.

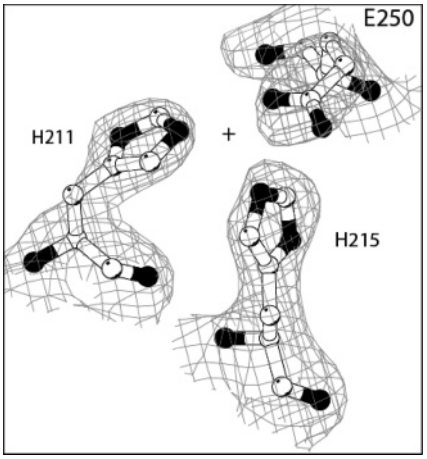


FIGURE 3: Composite omit map for Glu335Gln. Map contoured at 1$\sigma$. Zinc position corresponding to the wild-type structure is shown with a + sign for reference. There is no electron density corresponding to this in the Glu335Gln structure.

Table 4: Comparison of Interactions (Å) between Crucial Residues at the Active Site[a]

| as in wild type | wild type | R347A | E335A | E335Q | triple mutant | Y350A (B) |
|---|---|---|---|---|---|---|
| Zn−H211 NE2 | 2.18 | 2.30 | 2.36 | | 2.16 | 2.06 |
| Zn−H215 NE2 | 2.16 | 2.06 | 2.26 | | 2.26 | 2.11 |
| Zn−E250 OE1 | 2.22 | 2.24 | 3.79 | | 2.64 | 2.73 |
| Zn−E250 OE2 | 2.46 | 3.13 | 2.20 | | 2.06 | 2.40 |
| Zn−Nu wat | 2.17 | 2.60 | 2.47 | | 2.81 | 3.21 |
| Nu wat−E212 OE1 | 4.03 | 3.79 | 3.83 | 3.79 | 3.97 | 3.79 |
| Nu wat−E212 OE2 | 2.86 | 2.96 | 3.06 | 3.04 | 3.32 | 2.42 |
| Nu wat−Y350 OH | 3.58 | 3.53 | 4.44 | 2.90 | 3.92 | |
| Nu wat−E250 OE1 | 3.15 | 3.86 | 3.84 | 3.00 | 3.58 | 4.47 |
| Nu wat−R347 NH2 | 7.06 | | 7.01 | 7.16 | 7.70 | 7.80 |
| Nu wat−E250 OE2 | 3.66 | 4.02 | 3.86 | 3.19 | 4.14 | 5.32 |
| Nu wat−H215 NE2 | 3.74 | 4.04 | 4.35 | 3.29 | 4.41 | 4.54 |
| E335OE1−H211 ND1 | 2.61 | 2.52 | | 2.99 | 2.59 | 2.59 |
| E335 OE2−R347 NH1 | 2.99 | | | 3.39 | 2.94 | 3.13 |
| E249 OE1−H215 ND1 | 2.76 | 2.79 | 2.93 | 2.85 | 3.01 | 3.10 |
| E249 OE1−H218 ND1 | 2.73 | 2.69 | 2.73 | 2.80 | 2.97 | 2.82 |
| Y350 OH−Zn | 3.94 | 3.99 | 4.87 | | 4.05 | |
| Y350 OH−E250 OE1 | 3.15 | 3.38 | 3.66 | 3.48 | 3.69 | |
| Y350 OH−E250 OE2 | 3.43 | 3.76 | 3.63 | 3.80 | 3.53 | |
| R347 NH2−Zn | 7.08 | | 7.07 | | 7.19 | 7.01 |

[a] The two molecules in the asymmetric unit are identical within experimental error (RMSD = 0.8 Å), and accordingly, the interactions for monomer A are given for all structures except for Y350A. The nucleophilic water is displaced by a sulfate ion at the active site of monomer A in Y350A while B retains the water. Thus, for Y350A, interactions in molecule B are given. Nu wat is nucleophilic water.

*(E) Glu158Ala/Thr159Ala/Asn160Ala, a Triple Mutant.* These residues were considered on the basis of our modeling of the transition state in BoNT/B and the thermolysin structure (*29*). The active sites of thermolysin and BoNT/E-LC are similar though with some differences. Asn112 and Ala113 of thermolysin, which make contact with the scissile

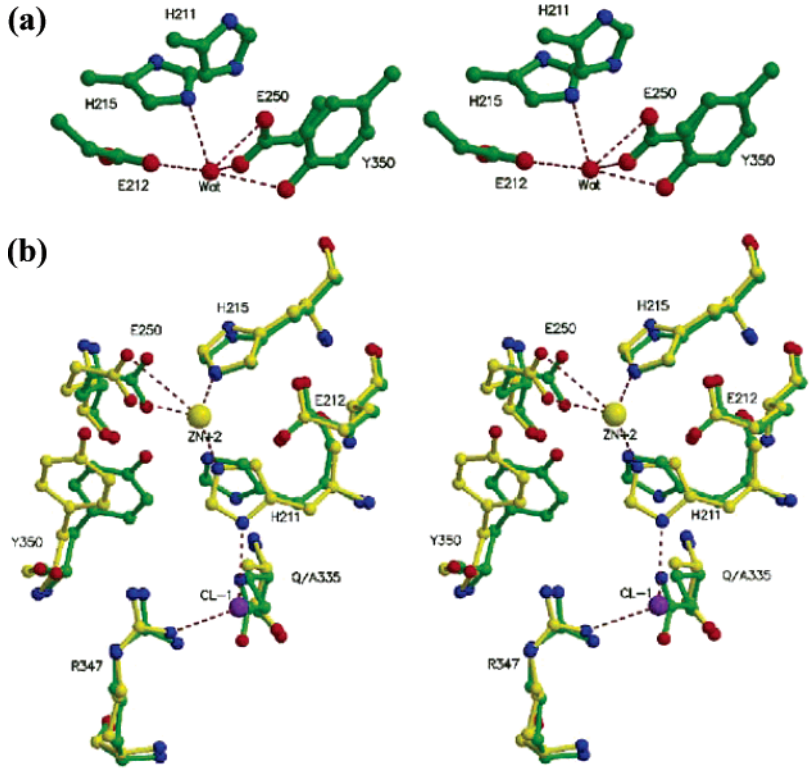


FIGURE 4: (a) Stereoview of the active site residues in Glu335Gln. The active site zinc is absent in this structure. The nucleophilic water has moved and makes strong hydrogen bonds with His211, Glu212, Glu250, and Tyr350. (b) Stereoview of the superposition of Glu335Ala (yellow) and Glu335Gln (green). The zinc ion corresponding to Glu335Ala is also shown in yellow and the chlorine ion in purple. Nucleophilic water molecules of the two structures are not shown for clarity. The change in orientation of His211 is apparent in the figure.

bond nitrogen, are positioned similarly to Glu158 and Thr159 in BoNT/E. Moreover, Glu158, a charged group, is <10 Å from the catalytic center. On the basis of these facts the triple mutant was constructed. The catalytic activity decreased by ~7-fold only. The crystal structure showed that the conformation of the active site is maintained but the nucleophilic water moved to hydrogen-bonding distance from zinc (2.81 Å) (Figure 2d). In the case of the triple mutant, since the hydrogen bond with the scissile peptide bond nitrogen is from the main chain O of Thr159, the activity decreases because of the loss of surface charge on Glu158Ala.

*Implications on the Catalytic Mechanism. (A) Arg347 and Tyr350 Stabilize the Substrate Binding.* In Arg347Ala, except for the movement of nucleophilic water, there is no major change in the active site conformation though the activity of the mutant is reduced 1000-fold. The effect is thus 13 times larger than that observed for the corresponding mutation in BoNT/A (*13*). It has been suggested that the arginine residue corresponding to Arg347 could be polarizing the nucleophilic water based on an inhibitor binding in thermolysin (*31*). However, in the present study, the low activity suggests that it may not be playing the role of polarizing the nucleophilic water, which is also supported by similar observations in BoNT/A-LC (*13*). The drastic reduction in activity without an accompanying structural change suggests that it plays an important role in substrate stabilization.

When the LC separates from the holotoxin, the loops rearrange and bring Tyr350 closer to the active site (*4*, *28*). The hydroxyl group of Tyr350 is 3.94 and 3.58 Å from zinc and the nucleophilic water, respectively, in the wild-type BoNT/E-LC (*3*). In addition to the hydroxyl group of Tyr350 being at hydrogen-bonding distance from the nucleophilic water, the aromatic−anionic interaction between Tyr350 and Glu250 helps to stabilize the position of Glu250. In BoNT/A, the reduction in activity of Tyr365Phe may be due to the loss of hydrogen-bonding interaction between the OH group and the nucleophilic water. In the BoNT/E-LC mutant Tyr350Ala, the complete loss of activity is due to the loss of both interactions. The side chain of Glu250 moves considerably, affecting the overall interactions with other active site residues. In TeNT the loss of activity for Tyr375Ala may be due to similar reasons. The reason for residual activity in the BoNT/A mutant Tyr365Ala is not clear (*14*). It may be because of some unidentified interaction compensating for the lost interaction. In our earlier study with Glu212Gln, which completely abolished the activity, we concluded that the proton donor must be Glu212 as in thermolysin (*3*). While mutation of Glu212 in BoNT/E and Glu224 in BoNT/A abolished the activity completely, the result of mutation of Tyr350 depends on the kind of mutation. Since the absence of the hydroxyl group (Tyr350Phe) only reduces the activity, Tyr350 may be providing the stabilizing force rather than donating a proton to the leaving group. This conclusion is also similar to that in thermolysin where the equivalent His231 plays a similar role (*21*).

Catalysis is a three-step process: the substrate recognition, docking to the active site, and the cleavage at a specific peptide bond. The optimal docking will bring about the maximum cleavage. The catalysis will be affected on the basis of the relative contribution of a particular residue in actual docking/stabilization of the substrate to the active center. We have shown that substitution of Tyr350 with Ala abolishes the catalysis, revealing the importance of this

residue in catalysis. The results suggest that the interactions of the carbonyl oxygen to the zinc and the Tyr350 are crucial for transition state stabilization. The hydroxyl group of this residue has been proposed to be the one involved in donating a proton to the leaving amide group (*4*, *15*). But since the change of tyrosine to phenylalanine does not abolish the activity either in BoNT/A or in TeNT, it may not be the proton donor for the leaving group. In thermolysin and neprilysin the direct interactions of similar residues to the substrate have been proposed (*18*−*21*). We have also proposed previously that Glu212 must be directly involved in proton donation based on the mutation Glu212Gln, which abolishes the activity completely (*3*).

In the initial stages of catalysis the reactants have to pass through a transition state to bring about catalysis. The transition state is often the result of strain or distortion of the reactants to form the particular electronic structure needed for the proper collision and product formation. Therefore, we propose that though the absence of Tyr350 may not affect the substrate docking severely (as seen by our competitive binding study), it is unable to provide the energy required to sustain the strain or distorted state needed for the catalysis, and hence the cleavage of the scissile bond is severely affected.

It is also not clear why the $K_m$ remains the same for Tyr350Ala and Arg347Ala if their role is for substrate stabilization. One explanation is that the loss of one interaction is compensated by another interaction (*19*). However, further studies with inhibitor molecules with mutants are needed to understand this more thoroughly.

*(B) Glu335Gln Is an Apoenzyme.* Despite the absence of zinc, there was some residual cleavage at high concentration (500 nM) of the mutant enzyme. It is not clear how a zinc endopeptidase devoid of zinc could still have some residual activity. One explanation is that the presence of nucleophilic water and its strong hydrogen-bonding interactions could still help in attacking the carbonyl carbon of the scissile bond. Or, Glu212, which is strongly hydrogen bonded to the nucleophilic water, could still act as a base, polarize the nucleophilic water, and attack the carbonyl carbon without the help of the zinc ion. This is similar to the Glu144Ser active site mutant of the *Bacillus cereus* thermolysin-like neutral protease where albeit in the absence of a charged base some residual activity was detected and attributed to the nucleophilic water molecule strongly hydrogen bonded to Ser144, a neutral amino acid (*32*). However, while the zinc ion was still present in that structure, it is absent in Glu335Gln. Another explanation for the residual activity could be the presence of traces of zinc in the assay buffer solutions, but we have shown that adding increasing amounts of zinc to the assay buffer does not change the (in)activity. In view of this Glu335Gln, an enzyme without the cofactor zinc, should be considered an apoenzyme, a persistent one in that it cannot bind zinc anymore. Even though we have shown that Glu212Gln is completely inactive, we constructed a double mutant Glu212Gln/Glu335Gln which will be both inactive and apoenzyme devoid of zinc. As expected, this double mutant had no activity whatsoever.

The extremely low catalytic efficiency (~7000-fold less) shown by the mutation Glu335Gln along with it being an apoenzyme (devoid of zinc) is baffling. The data are also supported by similar biochemical results obtained with BoNT/A-LC. Mutating the corresponding residue in BoNT/A to Ala/Gln led to drastic loss of activity and lowering of zinc content. The lower thermal stability observed in BoNT/A for this mutation may be due to the loss of zinc (*13*). Lowering of thermal stability has also been observed for apo BoNT/A-LC (*33*). When Glu is changed to Gln, the net charge changes by 1. This affects both the attractive and repulsive forces with the neighboring residues. Since the total electrostatic potential at any point is due to the sum total of all these changes, the environment must have changed. The change of interaction between this residue and the acidic residues would have caused this change. This is a classic example of how a subtle change in electrostatic properties (Glu is charged while Gln is neutral) can cause a major change in the environment. When the electrostatic potential surfaces of the wild-type enzyme are compared to those of mutant structures, it was clear that the electrostatic potential near Gln335 has changed considerably (data not shown). It is puzzling that Glu335Ala retains zinc and consequently more activity than Glu335Gln. The change in charge is the same except that the side chain of Gln335 can interact with surrounding residues unlike Ala335, resulting in different charge distribution in this region. The difference in orientation of His211 in Glu335Ala and Glu335Gln is shown in Figure 4b. The orientation of His211 in wild type is closer to Glu335Ala than Glu335Gln. This is probably because of the presence of a chlorine ion in the Glu335Ala mutant in the position of the side chain carboxylate group of Glu335 of wild type. It makes contacts with Arg347 NH2 and His211 ND1 at distances 3.27 and 3.34 Å, respectively. The reduction in activity may be partly because Tyr350 moves away from the active site (Table 4). The change in conformation and protonation of His211 may be a dominant factor for drastic reduction in Glu335Gln.

*(C) Position of Nucleophilic Water Is Crucial for Activity.* Movement of nucleophilic water is common to all mutant structures where decreased or loss of activity is observed. In Tyr350Ala and Arg347Ala the water position changes, contributing to the loss of activity. A similar observation has been made with Glu212Gln also (*3*). In Glu335Gln, despite the absence of zinc, the nucleophilic water is retained and makes stronger hydrogen bonds with active site residues, probably leading to some residual activity. In the triple mutant and Glu335Ala the movement of nucleophilic water is accompanied by a decrease in catalytic activity.

*Structural Comparison of BoNT/E-LC to Thermolysin and Neprilysin. Clostridium botulinum* neurotoxins, thermolysin, and neprilysin all belong to a metallopeptidase family with the zinc-binding motif HExxH+E. The distance between the HExxH motif and the second E varies. But it is informative to compare the three-dimensional structures of these three proteins to bring out similarities and differences. Even though the overall structures are different, the active site geometry is very similar in all of them. To compare the active sites of these three proteins, the residues in the zinc-binding motif (His, Glu, and His) were superposed (Figure 5). It has been hypothesized that His231 of thermolysin might correspond to Arg347 of BoNT/E, but the active site superposition shows that His231 is closer to Tyr350 than Arg347, in agreement with a recent analysis (*7*). The OH group of Tyr350 makes a close contact with the nucleophilic water (and also with the active site zinc). A similar contact is observed in

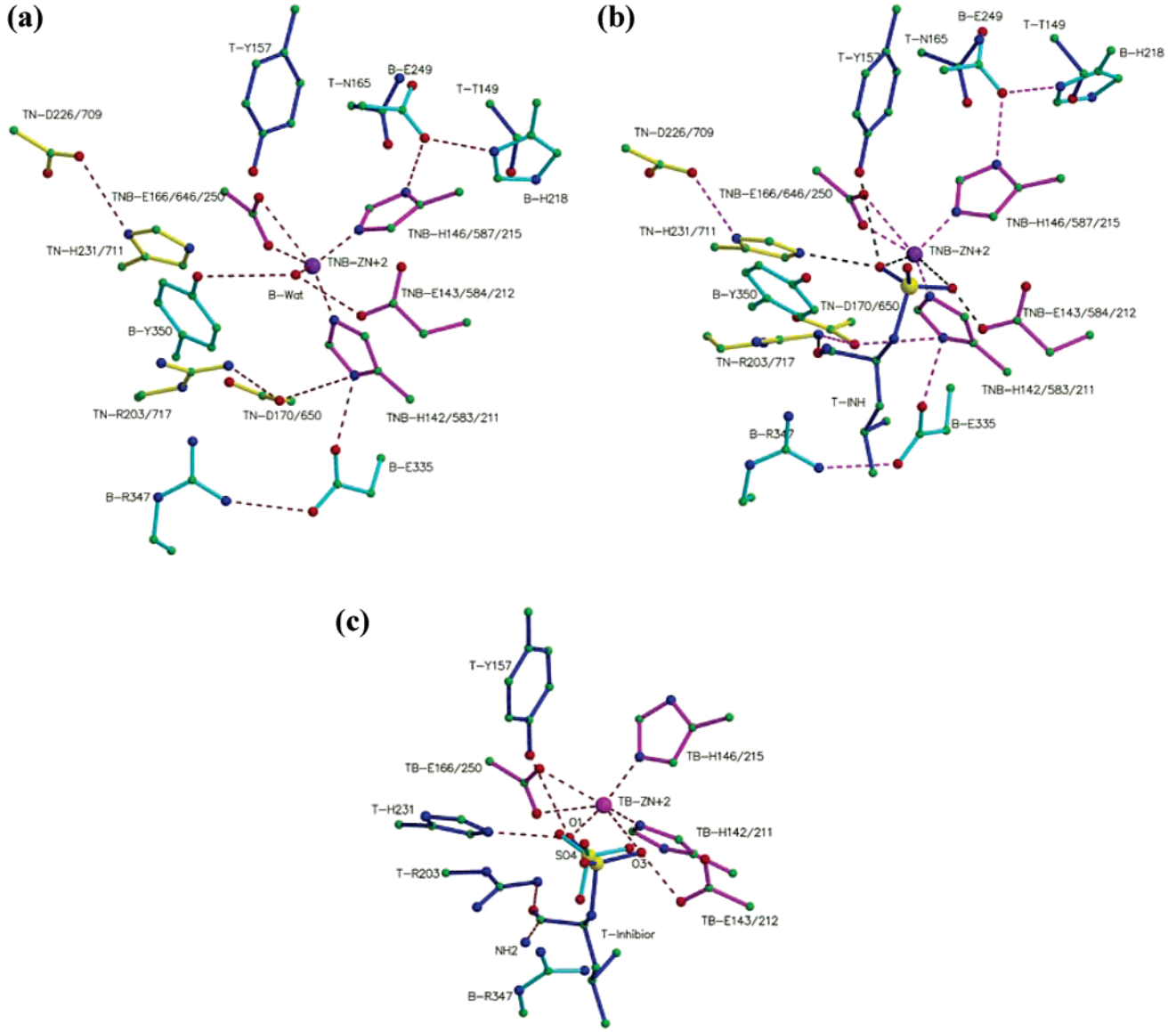


FIGURE 5: Superposition of the active sites of BoNT/E-LC, thermolysin, and neprilysin. Residues coordinating with zinc alone are considered for least-squares fit. (a) Residues common to all three proteins are in magenta and labeled TNB (thermolysin, neprilysin, and BoNT). Residues common to thermolysin and neprilysin (TN) are shown in yellow. BoNT (B) residues are in cyan. Tyr157 (T) which has no corresponding residue in the other two is shown in blue. For clarity only one of the common residues is shown, and the main chain atoms are omitted to avoid cluttering. Carbon, nitrogen, and oxygen atoms are in green, blue, and red, respectively. It is apparent that Tyr350 (B) corresponds to His231/His711 (TN). The hydrogen bond network from Arg203/717 (TN) is similar to that from Arg347 (B). Tyr157 (T) seems to be unique. Detailed comparison is given in the text. (b) As in (a) but shown with the transition state analogue inhibitor molecule of thermolysin (T, in blue) to highlight the interactions. This figure was produced with MOLSCRIPT and Raster3D (*34*). (c) Superposition of the active sites of molecule A of Tyr350Ala and thermolysin with an inhibitor. Residues common to thermolysin (T) and BoNT/E (B) are shown in magenta (for clarity only one of the common residues is shown). Residues of T are in dark blue, and residues of B and the sulfate ion are in cyan. Dotted lines represent coordination or hydrogen bond distances. Carbon, nitrogen, and oxygen atoms are in green, blue, and red, respectively. The sulfate ion positioned and oriented similarly to the phosphate group of the inhibitor in the thermolysin structure (PDB ID 2TMN) provides a model for substrate docking and transition state.

thermolysin (His231) and neprilysin (His711). Arg347 takes part in a hydrogen-bonded network connecting Glu335 and His211 in BoNT/E. Arg203 of thermolysin and Arg717 of neprilysin have a similar network with Asp170 and His142 and with Asp650 and His583, respectively. In view of this Arg347 should play a role similar to Arg203 or Arg717 and Glu335 that of Asp170 or Asp650. Indeed, the effect of mutation on Arg (1000-fold reduction) in botulinum is very similar to that observed in thermolysin and neprilysin (*19*). When Asp170 in thermolysin was changed to Ala, the specific activity decreased 220-fold. When Glu335 which serves a similar purpose in botulinum was changed to Ala, the activity decreased by ~40-fold. However, a mutation similar to Glu335Gln was not done for thermolysin. In thermolysin and neprilysin Asp226 and Asp709 provide stabilizing interactions for His231 and His711. The effect of mutating this Asp was not the same for thermolysin and neprilysin. There is no corresponding residue in botulinum. The reduction in activity due to mutating Tyr350 in botulinum depends on the nature of the mutation, suggesting that it needs both the phenolic ring and the hydroxyl group. Also, Tyr157, which makes a close interaction with nucleophilic water in thermolysin, has no counterpart either in botulinum or in neprilysin. Tyr157 in thermolysin may probably provide

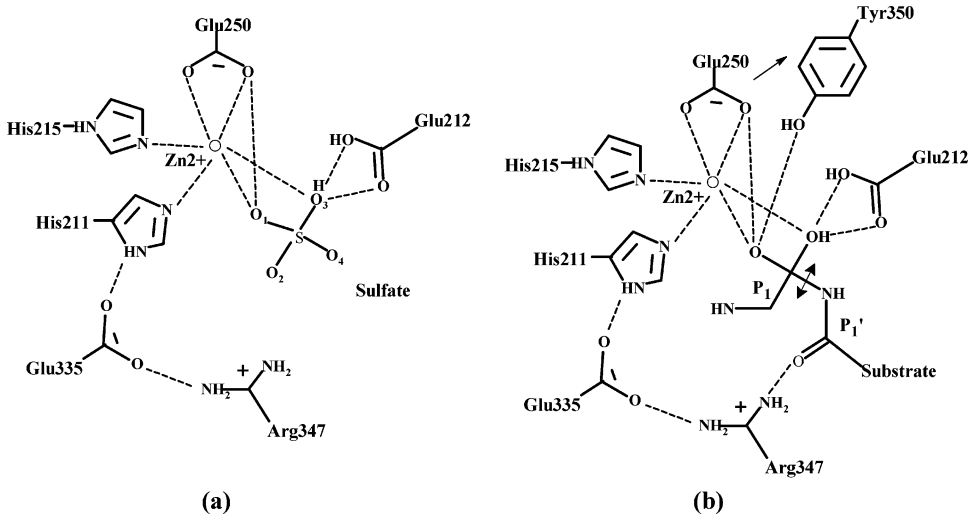


FIGURE 6: Proposed docking of substrate at the active site based on the interactions of the sulfate ion bound to the Tyr350 mutant molecule A and inhibitor-bound thermolysin (2TMN). (a) O1 of the sulfate ion at a distance of 2.4 Å from zinc corresponds to the carbonyl oxygen of the scissile bond (P1) while O3 corresponds to the nucleophilic water which moves closer to Glu212 but is still interacting with zinc. O2 and O4 will correspond to the Cα and scissile bond nitrogen. Thus the sulfate ion mimics the tetrahedral transition state of the substrate. (b) Proposed interactions of the carbonyl oxygens of P1 and P1′ of the substrate during the catalytic pathway. Tyr350 OH interacts with the P1 carbonyl oxygen while the Arg347 NH2 hydrogen bonds with P1′ stabilizing the substrate docking. An arrow mark between Glu250 and Tyr350 represents the anionic−aromatic interaction. The scissile bond is marked with a double-headed arrow mark.

extra stabilizing interactions since the effect of mutating this residue was considerably less than when His231 was mutated (*21*). Though these residues in the secondary coordination sphere are not exactly in the same position in space with respect to zinc, they provide the same kind of interactions and accordingly suggest that the catalytic mechanism of all three will be similar.

*Comparison of Tyr350Ala Molecule A with the Thermolysin−Inhibitor Complex.* The superposition of molecule A of Tyr350Ala on the structure with the thermolysin−inhibitor complex model shows interesting similarity (Figure 5c). The sulfate ion superimposes on the phosphate ion of the inhibitor very well and has similar interactions. The sulfate ion mimics the transitional tetrahedral geometry of the scissile peptide bond carbonyl carbon as in the case of the BoNT/B structure with a sulfate ion (*29*). The sulfur atom of sulfate imitates the carbonyl carbon of the scissile bond. O1 and O3 of the sulfate ion at distances 2.40 and 2.61 Å from zinc respectively mimic the positions of the scissile peptide bond carbonyl oxygen and displaced nucleophilic water. The O3 of sulfate makes hydrogen bonds with Glu212 OE1 and OE2 at 2.80 and 2.53 Å, respectively, and the O1 of sulfate with Glu250 OE1 at a distance of 2.84 Å. O4 of the sulfate represents the amide nitrogen of the scissile bond which is in hydrogen-bonding distance to Glu159 O as in thermolysin (Figure 6). This comparison also helps in mapping the S1′ subsite where P1′ (Ile181) of the substrate will bind. The side chain of P1′ occupies a cavity lined by Thr159, Phe191, Gln203, Leu207, Thr208, and Tyr356. The molecular surface in this region is shown in Figure 7.

From the models of thermolysin and neprilysin with their inhibitors it is proposed that Tyr350 and Arg347 interact with the carbonyl oxygens of P1 and P1′ of the substrate (here SNAP-25). When these interactions are not available, the catalytic activity is affected. This model could not be directly compared with the BoNT/A-SNAP-25 complex, since the scissile bond carbonyl oxygen is >6.5 Å away from zinc, maybe because of the absence of Tyr required for stabilization of the substrate (*7*). The overall comparison suggests that the substrate docking at the active site as well as the orientation of the peptide bond may be similar in all botulinum neurotoxins and tetanus neurotoxin even though the substrate and scissile bonds are different.

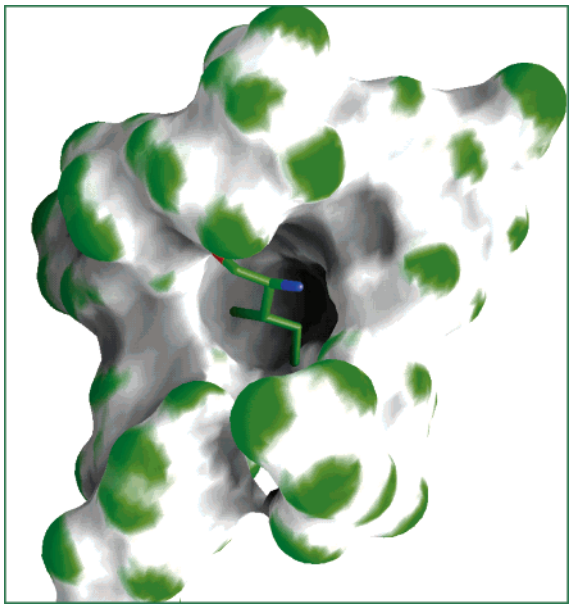

FIGURE 7: The molecular curvature surface formed by residues lying within 5 Å radius from P1′ (Ile181 of the substrate) is shown. The cavity occupied by the side chain of P1′ is lined by Thr159, Phe191, Gln203, Thr208, and Tyr356. Ile181 of the substrate alone is shown as a rod model. This figure was generated with GRASP (*35*).

## CONCLUSION

Overall, this study identifies the crucial role of nucleophilic water's presence, position, and polarizing ability. Since its position is determined by the conserved residues in the active site, an effective inhibitor common to all BoNTs can be

designed to block these conserved residues in combination. In this report we have also shown that subtle changes in the electrostatic potential due to changes on surface charges distant from the active site could drastically change the environment and the activity of the enzyme without altering the conformation. Glu335Gln is a persistent apoenzyme and could be a candidate for a recombinant vaccine. The double mutant Glu212Gln/Glu335Gln or Glu212Gln/Tyr350Ala could be a better target since both will be completely inactive with the former devoid of zinc. The residual activity on Glu335Gln also points to the fact that the nucleophilic water could still be attacking the scissile peptide bond carbonyl carbon in a way that is yet to be understood. In summary, we have shown that Arg347 and Tyr350 play a crucial role in substrate stabilization while Glu249 plays a supportive role in catalysis. Glu335, though in the secondary coordination sphere, plays a dominant role in changing the environment of the active site and the catalytic activity.

## ACKNOWLEDGMENT

We thank Drs. A. Saxena and M. Becker for providing beam time at the National Synchrotron Light Source, Brookhaven National Laboratory, J. Romeo for technical assistance, and Drs. S. Eswaramoorthy and D. Kumaran for helpful discussions.

## REFERENCES

1. Sollner, T., Whiteheart, S. W., Brunner, M., Erdjument-Bromage, H., Geromanos, S., Tempst, P., and Rothman, J. E. (1993) SNAP receptors implicated in vesicle targeting and fusion, *Nature 362*, 318−324.
2. Schiavo, G., Matteoli, M., and Montecucco, C. (2000) Neurotoxins affecting neuroexocytosis, *Physiol. Rev. 80*, 717−766.
3. Agarwal, R., Eswaramoorthy, S., Kumaran, D., Binz, T., and Swaminathan, S. (2004) Structural analysis of botulinum neurotoxin type E catalytic domain and its mutant Glu212→Gln reveals the pivotal role of the Glu212 carboxylate in the catalytic pathway, *Biochemistry 43*, 6637−6644.
4. Hanson, M. A., and Stevens, R. C. (2000) Cocrystal structure of synaptobrevin-ll bound to botulinum neurotoxin type B at 2.0 Å resolution, *Nat. Struct. Biol. 7*, 687−692.
5. Rao, K. N., Kumaran, D., Binz, T., and Swaminathan, S. (2005) Structural studies on the catalytic domain of clostridial tetanus toxin, *Toxicon* (in press).
6. Segelke, B., Knapp, M., Kadkhodayan, S., Balhorn, R., and Rupp, B. (2004) Crystal structure of *Clostridium botulinum* neurotoxin protease in a product-bound state: Evidence for noncanonical zinc protease activity, *Proc. Natl. Acad. Sci. U.S.A. 101*, 6888−6893.
7. Breidenbach, M. A., and Brunger, A. (2004) Substrate recognition strategy for botulinum neurotoxin serotype A, *Nature 432*, 925−929.
8. Lebeda, F. J., and Olson, M. A. (1995) Structural predictions of the channel-forming region of botulinum neurotoxin heavy chain, *Toxicon 33*, 559−567.
9. Kurazono, H., Mochida, S., Binz, T., Eisel, U., Quanz, M., Grebenstein, O., Wernars, K., Poulain, B., Tauc, L., and Niemann, H. (1992) Minimal essential domains specifying toxicity of the light chains of tetanus toxin and botulinum neurotoxin type A, *J. Biol. Chem. 267*, 14721−14729.
10. Rossetto, O., Schiavo, G., Montecucco, C., Poulain, B., Deloye, F., Lozzi, L., and Shone, C. C. (1994) SNARE motif and neurotoxins, *Nature 372*, 415−416.
11. Vaidyanathan, V. V., Yoshino, K., Jahnz, M., Dorries, C., Bade, S., Nauenburg, S., Niemann, H., and Binz, T. (1999) Proteolysis of SNAP-25 isoforms by botulinum neurotoxin types A, C, and E: Domains and amino acid residues controlling the formation of enzyme−substrate complexes and cleavage, *J. Neurochem. 72*, 327−337.
12. Washbourne, P., Pellizzari, R., Baldini, G., Wilson, M. C., and Montecucco, C. (1997) Botulinum neurotoxin A and E require the SNARE motif in SNAP-25 for proteolysis, *FEBS Lett. 418*, 1−5.
13. Binz, T., Bade, S., Rummel, A., Kollewe, A., and Alves, J. (2002) $Arg^{362}$ and $Tyr^{365}$ of the botulinum neurotoxin type A light chain are involved in transition state stabilization, *Biochemistry 41*, 1717−1723.
14. Rigoni, M., Caccin, P., Johnson, E. A., Montecucco, C., and Rossetto, O. (2001) Site-directed mutagenesis identifies active-site residues of the light chain of botulinum neurotoxin type A, *Biochem. Biophys. Res. Commun. 288*, 1231−1237.
15. Rossetto, O., Caccin, P., Rigoni, M., Tonello, F., Bortoletto, N., Stevens, R. C., and Montecucco, C. (2001) Active-site mutagenesis of tetanus neurotoxin implicates TYR-375 and GLU-271 in metalloproteolytic activity, *Toxicon 39*, 115−1159.
16. Yamasaki, S., Hu, Y., Binz, T., Kalkuhl, A., Kurazono, H., Tamura, T., Jahn, R., Kandel, E., and Niemann, H. (1994) Synaptobrevin/vesicle-associated membrane protein (VAMP) of *Aplysia californica*: structure and proteolysis by tetanus toxin and botulinal neurotoxins type D and F, *Proc. Natl. Acad. Sci. U.S.A. 91*, 4688−4692.
17. Li, L., Binz, T., Niemann, H., and Singh, B. R. (2000) Probing the mechanistic role of glutamate residues in the zinc-binding motif of type A botulinum neurotoxin light chain, *Biochemistry 39*, 2399−2405.
18. Matthews, B. W. (1988) Structural basis of the action of thermolysin and related zinc peptides, *Acc. Chem. Res. 21*, 333−340.
19. Marie-Claire, C., Ruffet, E., Antonczak, S., Beaumont, A., O'Donohue, M., Roques, B. P., and Fournie-Zaluski, M. C. (1997) Evidence by site-directed mutagenesis that arginine 203 of thermolysin and arginine 717 of neprilysin (neutral endopeptidase) play equivalent critical roles in substrate hydrolysis and inhibitor binding, *Biochemistry 36*, 13938−13945.
20. Marie-Claire, C., Ruffet, E., Tiraboschi, G., and Fournie-Zaluski, M. C. (1998) Differences in transition state stabilization between thermolysin (EC 3.4.24.27) and neprilysin (EC 3.4.24.11), *FEBS Lett. 438*, 215−219.
21. Beaumont, A., O'Donohue, M. J., Paredes, N., Rousselet, N., Assicot, M., Bohuon, C., Fournie-Zaluski, M. C., and Roques, B. P. (1995) The role of histidine 231 in thermolysin-like enzymes. A site-directed mutagenesis study, *J. Biol. Chem. 270*, 16803−16808.
22. de Kreij, A., van den Burg, B., Venema, G., Vriend, G., Eijsink, V. G., and Nielsen, J. E. (2002) The effects of modifying the surface charge on the catalytic activity of a thermolysin-like protease, *J. Biol. Chem. 277*, 15432−15438.
23. Agarwal, R., Eswaramoorthy, S., Kumaran, D., Dunn, J. J., and Swaminathan, S. (2004) Cloning, high level expression, purification and crystallization of the full length *Clostridium botulinum* neurotoxin type E light chain, *Protein Expression Purif. 34*, 95−102.
24. Otwinowski, Z., and Minor, W. (1997) Processing of X-ray diffraction data collected in oscillation mode, *Methods Enzymol. 276*, 307−326.
25. Brunger, A. T., Adams, P. D., Clore, G. M., Delano, W. L., Gros, P., Grosse-Kunstleve, R. W., Jiang, J. S., Kuszwewski, J., Nilges, M., Pannu, N. S., Read, R. J., Rice, L. M., Somonsom, T., and Warren, G. L. (1998) Crystallography & NMR system: a new software suite for macromolecular structure determination, *Acta Crystallogr. D54*, 905−921.
26. Jones, T. A., Zou, J., Cowtan, S., and Kjeldgaard, M. (1991) Improved methods in building protein models in electron density map and the location of errors in these models, *Acta Crystallogr. A47*, 110−119.
27. Lipscomb, W. N., and Strater, N. (1996) Recent advances in zinc enzymology, *Chem. Rev. 96*, 2376−2433.
28. Swaminathan, S., and Eswaramoorthy, S. (2000) Structural analysis of the catalytic and binding sites of *Clostridium botulinum* neurotoxin B, *Nat. Struct. Biol. 7*, 693−699.
29. Swaminathan, S., Eswaramoorthy, S., and Kumaran, D. (2004) Structure and enzymatic activity of botulinum neurotoxins, *Movement Disorders 19* (Suppl. 8), S17−S22.

30. Eswaramoorthy, S., Kumaran, D., Keller, J., and Swaminathan, S. (2004) Role of metals in the biological activity of *Clostridium botulinum* neurotoxins, *Biochemistry 43*, 2209−2216.
31. Mock, W. L., and Aksamawati, M. (1994) Binding to thermolysin of phenolate-containing inhibitors necessitates a revised mechanism of catalysis, *Biochem. J. 302*, 57−68.
32. Lister, S. A., Wetmore, D. R., Roche, R. S., and Codding, P. W. (1996) E144S Active-site mutant of the *Bacillus cereus* thermolysin-like neutral protease at 2.8 Å Resolution, *Acta Crystallogr. D52*, 543−550.
33. Li, L., and Singh, B. R. (2000) Role of zinc binding in type A botulinum neurotoxin light chain's toxic structure, *Biochemistry 39*, 10581−10586.
34. Kraulis, P. J. (1991) MOLSCRIPT: a program to produce both detailed and schematic plots of proteins, *J. Appl. Crystallogr. 24*, 946−950.
35. Nicholls, A., Sharp, K., and Honig, B. (1991) Protein folding and association: insights from the interfacial and thermodynamic properties of hydrocarbons, *Proteins 11*, 281−296.

BI050253A